Kinetics and Catalysis, Vol. 42, No. 3, 2001, pp. 390–398. Translated from Kinetika i Kataliz, Vol. 42, No. 3, 2001, pp. 432–441.

IV RUSSIAN CONFERENCE WITH THE PARTICIPATION OF CIS COUNTRIES ON THE SCIENTIFIC BASES OF CATALYST PREPARATION AND TECHNOLOGY

Scientific Bases for the Synthesis of Highly Dispersed Framework Zirconium Phosphate Catalysts for Paraffin Isomerization and Selective Oxidation

V. A. Sadykov[1], S. N. Pavlova[1], G. V. Zabolotnaya[1], M. V. Chaikina[3], R. I. Maksimovskaya[1], S. V. Tsybulya[1], E. B. Burgina[1], V. I. Zaikovskii[1], G. S. Litvak[1], Yu. V. Frolova[2], D. I. Kochubei[1], V. V. Kriventsov[1], E. A. Paukshtis[1], V. N. Kolomiichuk[1], V. V. Lunin[4], N. N. Kuznetsova[4], D. Agrawal[5], and R. Roy[5]

[1]*Boreskov Institute of Catalysis, Siberian Division, Russian Academy of Sciences, Novosibirsk, 630090 Russia*

[2]*Novosibirsk State University, Novosibirsk, 630090 Russia*

[3]*Institute of Solid-State Chemistry and Mechanochemistry, Siberian Division, Russian Academy of Sciences, Novosibirsk, 630128 Russia*

[4]*Department of Chemistry, Moscow State University, Moscow, 117234 Russia*

[5]*Materials Research Laboratory, Pennsylvania State University, University Park, PA, USA*

Received September 18, 2000

Abstract—Results of the systematic study of the synthesis of highly dispersed framework zirconium phosphates stabilized by ammonium, lanthanum, aluminum, manganese, and cobalt cations are summarized. The synthesis involves the mechanochemical activation of a mixture of solid reactants (salts) or the sol–gel process each followed by the hydrothermal treatment (HTT) of obtained precursors in the presence of surfactants. The genesis of dispersed systems under investigation is studied by modern physical methods providing information on the state of the bulk and surface of the systems. It is found that the local structure of sol nanoparticles and zirconium phosphate crystalline nuclei arising from mechanochemical activation products depends on the nature of initial substances. This, in its turn, makes different crystallization mechanisms possible during the HTT process: the dissolution/precipitation mechanism or the mechanism of oriented mating of primary particles. The crystallization mechanism in HTT and the reaction system composition influence the nature of resulting complex zirconium phosphate phases, their thermal stability, dispersity, and porous structure parameters. The relationship between the bulk structure parameters of framework zirconium phosphates, which are controlled by varying the chemical composition and conditions of synthesis, and the surface characteristics of the systems (the strength and concentration of different Lewis and Brønsted sites) is studied. It is shown that systems based on framework zirconium phosphates are promising catalysts for paraffin (pentane and hexane) isomerization, the selective oxidation of methane by oxygen into synthesis gas at short contact times, and the oxidative dehydrogenation of propane into propylene.

INTRODUCTION

Currently, complex inorganic phosphates attract growing interest from specialists in the area of heterogeneous catalysis as promising catalytic systems in various acid (isomerization and hydration [1–3]) and redox (the selective oxidation of paraffins to olefins or oxygen-containing products [4–6]) processes. Among such systems, framework zirconium phosphates of the NASICON (NZP) type with the base composition $M_2Zr_4P_6O_{24}$ are of great interest owing to their flexible structure, which enables the heterovalent substitution at both cation and anion sites of the lattice without its destruction [7–10]. Materials based on these compounds have a high cation and proton conductivity; high resistance to irradiation and corrosion and extra low thermal expansion coefficients [11–13]. These properties make them suitable for radionuclide immobilization. The heterovalent substitution provides a means for varying the redox and acid–base properties of systems based on framework zirconium phosphates over broad limits. In addition to practical importance, this also makes these systems suitable for use as model objects in the development of scientific foundations for the synthesis of catalysts.

In this article, we discuss the genesis of highly dispersed systems based on framework zirconium phosphates with the chemical composition, the nature of initial substances, and synthesis conditions varied over broad limits.

A traditional method for synthesizing framework zirconium phosphates is the sol–gel (SG) process. Disadvantages of this method are the poor reproducibility of substance characteristics, the spatially nonuiniform distribution of components, and the frequent amor-

0023-1584/01/4203-0390$25.00

phous state of systems retained up to high annealing temperatures, at which the agglomeration results in materials with a low surface area. Therefore, in the development of methods for synthesizing highly dispersed systems based on framework phosphates, which are of interest for as commercial catalysts, in parallel with the traditional sol–gel method, we also used was the "soft" mechanochemical method involving the activation of a solid salt mixture in a high-energy mill [14]. Moreover, to reach the required dispersity and structure stability of systems based on framework zirconium phosphates and to provide a means for controlling their porous structure, the sols and mechanical activation (MA) products were subjected to hydrothermal treatment (HTT) [15, 16], in particular, in the presence of surfactants. This approach allowed understanding the genesis of these systems, including the structure of nanoparticles serving as nuclei of framework phosphates and the process of their mating to yield mesoscopic aggregates and then micron particles. At the present time, studies along theses lines are among the most intensively progressing fields in material science and solid-state chemistry.

Ammonium, lanthanum, aluminum, manganese, and cobalt cations were used for stabilizing the structure of framework zirconium phosphates.

The genesis of actual structures of zirconium phosphates at key synthesis stages was studied using modern physical methods of studying the structure and texture of nanoparticles, such as EXAFS, high-resolution transmission electron microscopy (HRTEM), ^{31}P and ^{27}Al MAS NMR, small-angle X-ray scattering (SAXS), and IR spectroscopy. The dependence of the surface characteristics of highly dispersed framework zirconium phosphates on their composition, bulk properties, and synthesis conditions was studied using the IR spectroscopy of adsorbed probe molecules (CO) and the ESR of spin probes (the TEMPO nitroxyl radical and aromatic molecules like benzene).

The catalytic activity of the systems was measured for the reactions of pentane and hexane skeletal isomerization, hexane dehydroaromatization, and methane selective oxidation into synthesis gas at short contact times.

The synthesis of samples and procedures of their investigation were described in detail earlier [17–28].

1. GENESIS OF THE STRUCTURE OF COMPLEX ZIRCONIUM PHOSPHATES

1.1. The Structure of Primary Particles

It was shown that even at the stage of mechanical activation of the solid salt mixture (the mixture of ammonium phosphates of different composition, zirconyl nitrate or chloride, and lanthanum, aluminum, manganese, and cobalt nitrates as stabilizers), crystalline hydrates are partially decomposed to yield a supersaturated solution film on solid particles. Reactant interaction in this heterogeneous system results in crystalline ammonium chloride or nitrate [20, 22]. Besides, the interaction between zirconium cations and phosphate groups results in primary products, whose structure depends in large measure on the nature of the initial ammonium salt. For example, with triammonium phosphate, the nuclei most probably correspond in their structure to arising fragments of lamellar phosphates. This is seen from the phosphorus NMR spectrum (Fig. 1) involving four equidistant bands in the chemical shift range from +1 to –15 ppm, which is indicative of stepwise changes in the cationic environment of phosphate during the reactant interaction. With diammonium phosphate, the spectrum of the MA product involves a broad band at –15.5 ppm characteristic of lamellar zirconium hydrophosphates [29]. With monoammonium phosphate, the spectrum (Fig. 1) involves a broad band at –25.7 ppm attributed to PO_4^{3-} groups in a symmetrical environment closely resembling that for high-temperature samples of framework zirconium phosphates with the NZP-like structure [17]. In agreement with these data, IR spectra of MA products obtained from mixtures based on hydrophosphates involve near-symmetrical bands in the range 1020–1050 cm^{-1} closely corresponding to those typical of amorphous samples obtained using the sol–gel process [21, 22]. At the same time, with triammonium phosphate, phosphate groups in arising structures have

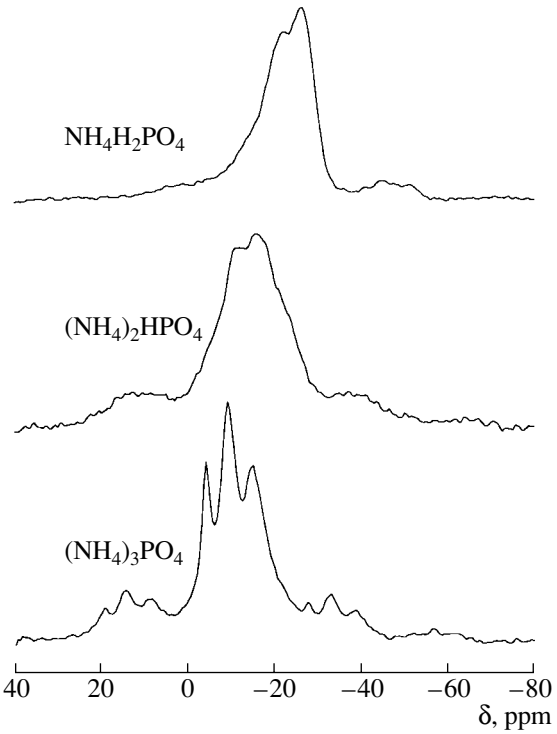

Fig. 1. ^{31}MAS NMR spectra of MA products obtained using ammonium phosphates of different composition.

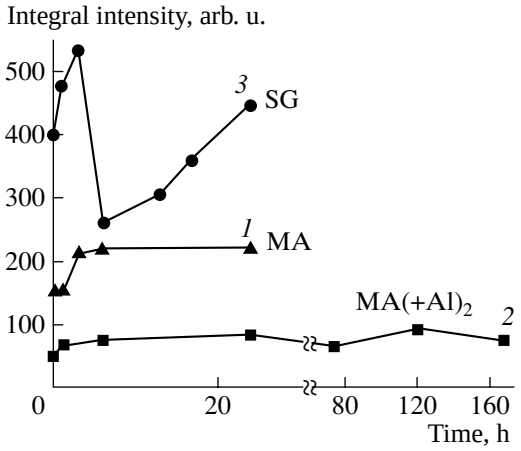

Fig. 2. Evolution of the integral intensity of small-angle X-ray scattering on particles of (*1*) MA products without admixed ions and (*2*) MA products with admixed Al^{3+} ions and also on (*3*) sol particles during their hydrothermal treatment at 175°C with polyethylene oxide aqueous solutions with pH 1 (SG) and 7 (MA products); the particle size is in the range 0–200 Å.

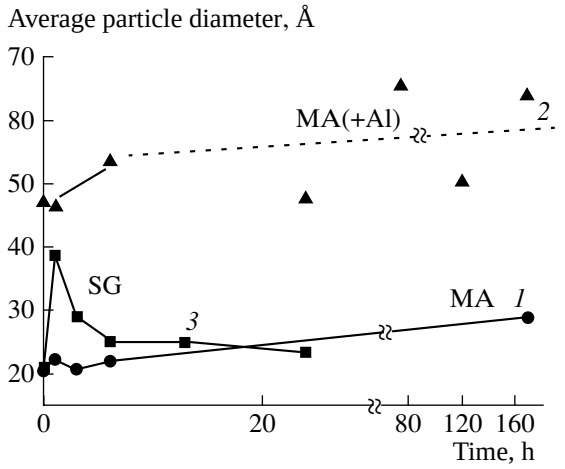

Fig. 3. Evolution of the average particle size (in the range 0–200 Å) for (*1*) MA products without admixed ions, (*2*) MA products with admixed Al^{3+} ions, and (*3*) sols during their hydrothermal treatment at 175°C with polyethylene oxide aqueous solutions with pH 1 (SG) and 7 (MA products).

a distorted tetrahedral coordination (the doublet at 1000–1100 cm^{-1}).

Thus, the use of hydrophosphates intensifies the reactant interaction during their mechanical activation probably due to the more intensive hydrolysis of hydroxyl bridges between zirconium cations in polymeric/oligomeric complexes present in the hydrated zirconium salt [30].

1.2. Crystallization during the Hydrothermal Treatment

It was found [20, 22] that, even at pH 7, the hydrothermal treatment of MA product aqueous suspensions (with or without polyethylene oxide (PEO)) obtained from neutral ammonium phosphate results in a crystalline product largely composed of cubic ammonium zirconium phosphate [31, 32] with admixed orthorhombic phases, such as β-$Zr(OH)PO_4$ or $Zr_2O(PO_4)_2$ [33]. The formation of crystalline phases in the conditions precluding the dissolution of MA primary products suggests that the crystallization occurs by the mechanism of the oriented mating of primary particles. At the same time, the fact that the MA products yield solely zirconium pyrophosphate upon mere annealing suggests that the hydrothermal treatment is accompanied not only by primary particle mating but also by a change in their structure.

In sols obtained by the coprecipitation of zirconium salts and ammonium phosphates from their solutions, crystalline phases arise only upon the hydrothermal treatment at 175–200°C in acidic media (pH~1). In this case, in the presence of PEO, along with α-$ZrPO_4(OH)$ [33, 34], the $NH_4Zr_2(PO_4)_3$ cubic phase was also found [22]. These results suggest that the sol crystallization occurs by the dissolution/precipitation mechanism. This is probably due to the hindered rearrangement of sol particles into the structure of framework phosphate nuclei under these conditions.

This conclusion was supported by data on the crystallization dynamics studied in detail by SAXS [21].

According to the SAXS data, before hydrothermal treatment, sol or MA product particles have a rather narrow size distribution, about 15 (MA) or 18 (SG) Å, and only a small proportion of particles is as large as 60–70 Å in diameter. However, during the heating and subsequent exposure at the treatment temperature, particle sizes in samples obtained by the MA and SG methods change quite differently. During the hydrothermal treatment of samples obtained by the MA method, in the particle size distribution curve, new maximums arise and are growing at 30, 45, 75, 105, 130, and 165 Å. All these sizes can be obtained by combining several primary particle sizes, which is evidence for the crystallization mechanism by oriented particle mating. This is also supported by the facts that the integral intensity of the small-angle X-ray scattering remains constant with the particle size varying in the range 0–200 Å (Fig. 2) and that the average particle size increases with time (Fig. 3).

The introduction of aluminum cations into the system subjected to activation markedly increases the average size of crystalline nuclei, which suggests that these cations are mostly localized in the second coordination sphere of oligomeric zirconium hydroxy complexes with phosphate groups in the first coordination sphere. The oriented crystallization in the system containing aluminum cations remains much the same; however, nonmonotonic changes with time in the average particle size and the integral intensity of the small-

angle scattering (Figs. 2 and 3) are indicative of a more complex nature of changes in the local structure of nuclei during HTT (see below).

The crystallization of sols in acidic media occurs in a different fashion. The heating of a suspension to 175°C is accompanied by the aggregation of sol primary particles giving rise to new maximums in the particle size distribution curve at 40, 70, 110, and 165 Å. During the subsequent hydrothermal treatment, all these maximums decrease and then disappear. A decrease in the average particle size (within the range 0–200 Å; Fig. 3) with time points to the dissolution of particles and their aggregates. However, the integral intensity of X-ray scattering on the sol particles shows more complex time dependence. The intensity initially increases probably due to the disintegration of large (larger than 200 Å) aggregates into small primary particles and then decreases due to the primary particle dissolution.

A better insight into the crystallization mechanism was gained using high-resolution electron microscopy, EXAFS, IR spectroscopy, and NMR on phosphorus and aluminum nuclei [21, 22]. It was shown that the mating of MA primary particles in neutral media occurs anisotropically to yield initially extended filaments as thick as primary particles. During the hydrothermal treatment, the filaments combine into ribbons and then into rather wide (to 250 Å) lamellas as long as several thousands of angströms. At the final stages of crystallization, lamellas are randomly superimposed to give isotropic particles of cubic ammonium zirconium phosphate or lamellar particles of the β-$Zr(OH)PO_4$ orthorhombic phase. We believe that the anisotropic mating of primary crystalline particles is due to the anisotropy of their properties, which might be expected to be characteristic of lamellar fragments similar in structure to lamellar phosphates (see the NMR data presented above). Indeed, basal planes in lamellar phosphates carry negatively charged phosphate groups [1], and their mating is excluded for electrostatic reasons. At the same time, lateral sides containing coordinatively unsaturated zirconium cations nonshielded by phosphate groups can participate in the primary particle mating. The mutual superposition of particles occurs only late in the hydrothermal treatment, when the three-dimensional structure of crystalline particles is rearranged into the framework structure of zirconium phosphates (see below).

The considered crystallization mechanism characteristic of neutral solutions suggests that the surface of cubic ammonium zirconium phosphate particles is largely composed of coordinatively unsaturated basal planes and, consequently, is dominated by phosphate groups. Indeed, this suggestion is supported by IR spectra of surface groups (see below).

Although the hydrothermal treatment of sols at pH 5–7 gives no crystalline phases detectable by XRD, the electron microscopy study of X-ray amorphous samples revealed needle-shaped crystalline particles with the morphology typical of the rhombohedral phase of ammonium zirconium phosphate [18, 19, 22]. This suggests a nonuniformity in the properties of sol particles due to the spatially nonuniform distribution of components both during the reactant interaction and in the resultant sol (gel), which is typical of the coprecipitation method. As a result, some sol particles may have surface characteristics similar to those for the MA products, which enables their oriented mating.

According to the EXAFS data [21], during the hydrothermal treatment of sols in acidic media up to the closing stage, the Zr–O, Zr–Zr, and Zr–P distances remain virtually constant ($R \sim 2.06$, 2.8, and 3.6 Å, respectively), as well as their corresponding coordination numbers. According to the data of MNR and IR spectroscopy, the characteristics of phosphate groups also remain unchanged. Thus, the crystallization of sols in acidic media is not accompanied by changes in their structure characteristics, specifically in coordination spheres of zirconium and phosphorus, which is consistent with the dissolution/precipitation mechanism. By contrast, during the hydrothermal treatment of MA products in neutral media, the zirconium–oxygen and zirconium–phosphorus coordination numbers monotonically increase, which is consistent with the model of oriented mating of primary particles [20, 22]. Moreover, a progressive change in characteristics of phosphate groups evident from ^{31}P NMR spectra (Fig. 4a) is indicative of an increase in the number of their coordinated multicharged (mostly zirconium) cations. Judging from EXAFS data, upon the hydrothermal treatment, the number of phosphate groups coordinated to a zirconium cation approaches six, which, at the given stoichiometry, suggests that each phosphate group in the bulk is coordinated to four zirconium cations.

Additional valuable information on the rearrangement of the atomic structure of primary particles during the crystallization of cubic zirconium phosphate from neutral solutions of MA products was obtained using NMR on aluminum nuclei (Fig. 4b). Data suggest that, in the MA product, aluminum cations are in at least two coordination environments—tetrahedral (the signal at +46 ppm) and distorted octahedral (–10 ppm)—similar to those for phosphated aluminum oxide [27]. As noted above, in nuclei produced by the MA method, phosphated aluminum cations are most likely to be located in the outer sphere of fragments with the structure of lamellar zirconium phosphates. During the hydrothermal treatment, the signal from the tetracoordinated aluminum cation first accumulates slightly, which can be assigned to a stronger interaction between aluminum and phosphate groups giving rise to the local structure of aluminum phosphates [27] and then, later in the hydrothermal treatment, the signal from the tetrahedral cation disappears, and the signal at a stronger field shifts to 20 ppm. This points to an increase in the coordination number of the substituent cation probably due to its introducing into the structure of cubic framework

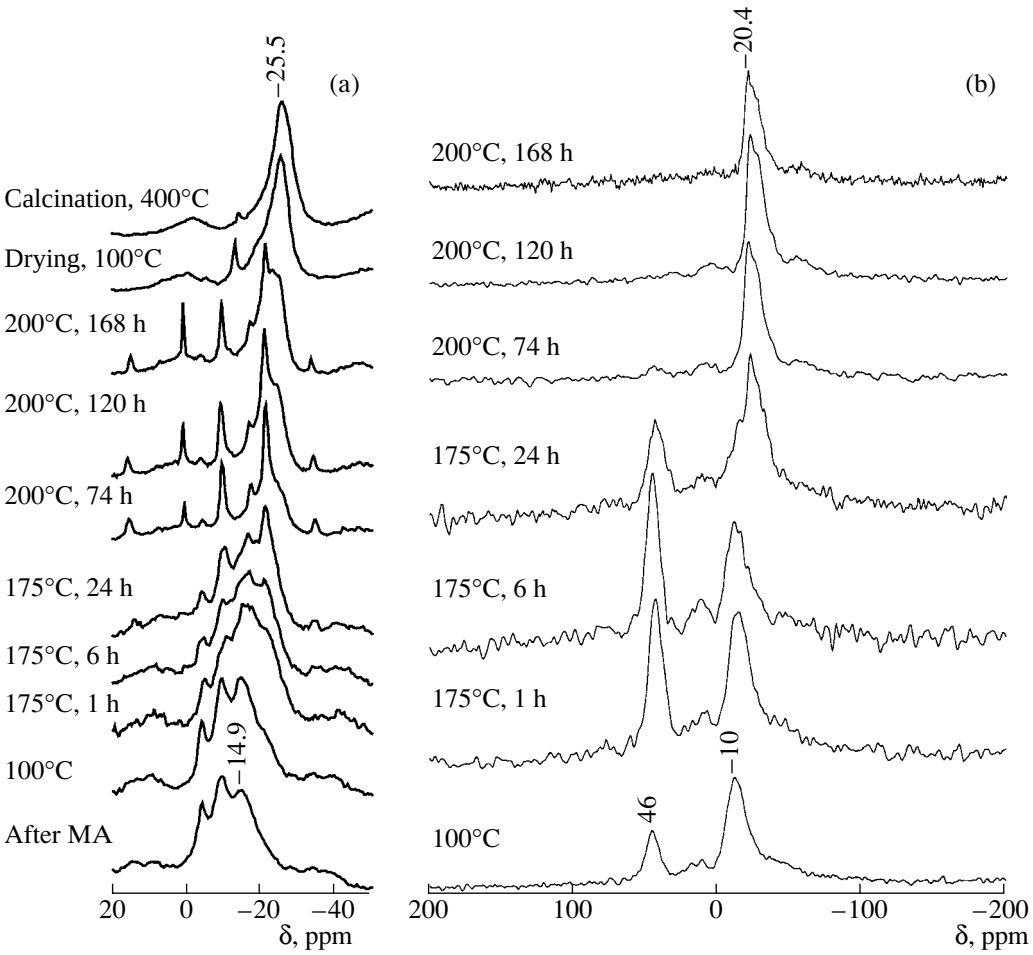

Fig. 4. Evolution of (a) ^{31}P and (b) ^{27}Al MAS NMR spectra of the aluminum-containing MA product during its treatment.

phosphate at the zirconium position or most likely at the position with a coordination number of nine in oxygen usually occupied by alkali or alkaline-earth cations.

1.3. The Influence of the Chemical Composition of the System and the Nature of Initial Salts on the Crystallization Process during the Hydrothermal Treatment and on the Nature and Stability of Resultant Phases

The schemes 1 and 2 illustrate the dependence of the nature of phases formed by the hydrothermal treatment of MA products and sols on their chemical composition, the nature of initial substances, and the synthesis conditions.

The influence of the nature of the initial zirconium compound. With zirconyl chloride as an initial substance, the samples obtained by HTT at pH 7 followed by annealing at 400°C contain much less admixed orthorhombic phase and zirconium pyrophosphate then the samples obtained under the same conditions from zirconyl nitrate. This finding is explained by the influence of the crystal matrix of the MA solid product (ammonium salts) on the structure of new nuclei. For example, the cubic structure of ammonium chloride favors the formation of cubic ammonium zirconium phosphates, whereas the orthorhombic structure of ammonium nitrate favors the formation of orthorhombic zirconium orthophosphate. A decrease in the zirconium pyrophosphate content of annealed samples is explained by the known inhibiting effect of chloride anions on the formation of condensed phosphates [35].

The addition of polyethylene oxide to MA product aqueous suspensions subjected to the hydrothermal treatment at neutral pH favors the formation of a cubic phase.

The addition of lanthanum and aluminum nitrates and ammonium fluoride to initial components exerts the same effect. The influence of lanthanum cations, taking into consideration their large size, can be assigned to their tendency to occupy positions with high coordination numbers present in the structure of cubic zirconium phosphate. However, similar influence of aluminum cations suggests that triple-charge cations can stabilize the cubic phase due to effects of

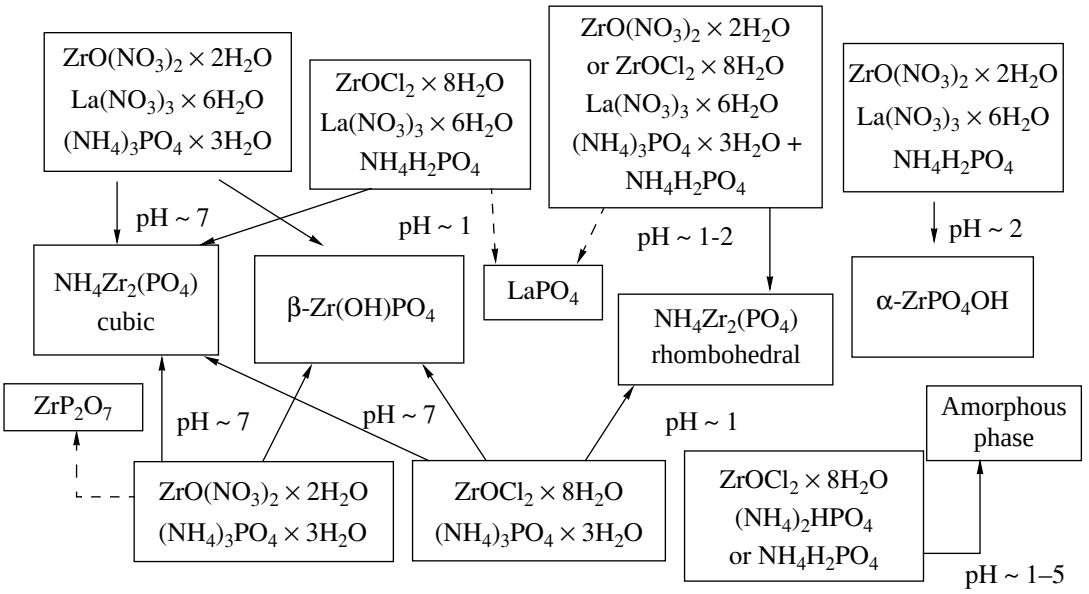

Scheme 1. The main types of phases obtainable by the hydrothermal treatment of MA products under different conditions.

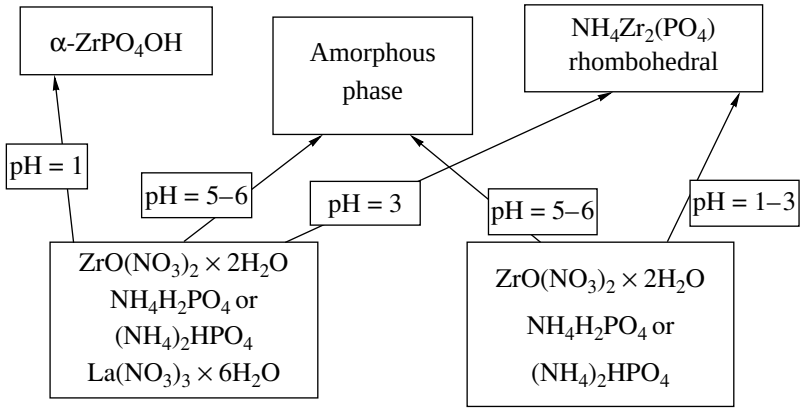

Scheme 2. Main types of phases obtainable by the hydrothermal treatment of sols in different conditions.

charge disordering of the system with these cations at zirconium positions. The charge balance in the lattice can be attained due to large hydroxonium cations additionally introduced into the lattice. The influence of fluoride anions can also be explained by the charge disordering but in the anionic sublattice.

The introduction of manganese and cobalt into zirconium phosphates produces the monoclinic distortion of their structure, most pronounced in samples annealed at a high (800–900°C) temperature favorable to the removal of residual water. According to EXAFS data, cobalt cations occupy positions with a low coordination number in oxygen (the cobalt–oxygen coordination number is ~4). The presence of a triplet (~15000, 17000, and 19000 cm^{-1}) in diffuse-reflectance electronic spectra, which is assigned to electronic transitions of Co^{2+} in a coordination of the tetrahedral type, agrees with the EXAFS data. This suggests that the distortion of the structure of framework zirconium phosphates due to the presence of cobalt is determined by its tendency to occupy positions with a low coordination number in oxygen. The structure distortion in manganese-containing samples is probably due to the same reason.

The influence of the nature of ammonium phosphates. On the hydrothermal treatment in acidic media, the MA products based on triammonium phosphate yield rhombohedral ammonium zirconium phosphate. The crystallization evidently occurs by the dissolution/precipitation mechanism.

The most interest finding is seemingly the fact that the hydrothermal treatment of MA products based on

the dihydrophosphate without admixed lanthanum is not accompanied by crystallization. At the same time, sol samples obtained from ammonium hydrophosphates are readily dissolved in acidic media (pH 1–3) to yield rhombohedral-framework phosphate or, in the presence of lanthanum, α-$ZrPO_4OH$. Thus, the absence of dissolution cannot be attributed solely to the nuclei composition. Note that, unlike the case with triammonium phosphate (see above), these nuclei differ in the structure from framework phosphates because of their stronger interaction with phosphate groups during the MA process. We believe that the use of ammonium hydrophosphates favors the preferred concentration of phosphate groups on the surface of crystalline nuclei arising in the solid salt (ammonium chloride or nitrate) matrix. This can be due to the binding of ammonium cations, which stabilize the structure of framework phosphates, in the solid salt (ammonium chloride/nitrate) matrix and the occupation of their sites in the lattice of nuclei by protons (hydroxonium cations). The result is the formation of a negatively charged layer on the particle surface, which prevents zirconium cations from passing into the acidic solution. In this context, the formation of crystalline phases from MA products also obtained from hydrophosphates but with admixed lanthanum is reasonably explained by an increased concentration of cations stabilizing the lattice of framework phosphates and, consequently, by a change in the negative surface charge for positive required for dissolution. In this case, judging from MNR spectra on phosphorus nuclei, bulk structure characteristics of crystalline nuclei with and without admixed lanthanum were virtually the same.

The morphology and the nature of phases produced by HTT in acidic media. The nature of crystalline phases produced by the hydrothermal treatment of sols or MA products depends on the cationic composition of the systems. Lanthanum, when present, favors the formation of the cubic phase or a phase of the α-$ZrPO_4OH$ type; this is explained by the fact that lanthanum tends to occupy positions with higher coordination numbers in oxygen, which are present in these structures.

The morphology of particles of rhombohedral ammonium zirconium phosphate was found to be strongly dependent on the method of preparing the initial X-ray amorphous system to be exposed to HTT in an acidic medium. The hydrothermal treatment of sols results in step-shaped crystalline particles arising by the oriented mating of thin rectangular lamellas as large as 500 Å with a well-developed prismatic face. Samples obtained by HTT of MA products largely composed of thicker lamellar particles typically 2000 Å in size with most-developed basal, prismatic, and rhombohedral faces. These seemingly unexpected findings from the standpoint of crystallization by the dissolution/precipitation mechanism can be explained as follows. It should be taken into consideration that a new crystalline phase can arise by the heterogeneous nucleation mechanism instead of the formation of critical nuclei, which is highly probable for sparingly soluble substances like zirconium phosphates. During the long-term HTT, sol or MA product particles with a higher degree of crystallinity and hence remaining unsolved can serve as nucleation centers in the formation of framework zirconium phosphates. In this case, it should be expected that the structure of nuclei and, consequently, the morphology of crystalline particles growing on them would depend on the history of the product subjected to HTT.

The thermal stability of framework zirconium phosphates. The stability of framework zirconium phosphates depends to a large measure on the presence of substituent ions in their structure. However, it should be noted that the cubic phase stabilized by ammonium cations and water holds its structure even upon calcination at 800–900°C accompanied by the removal of ammonia and water [18]. A plausible explanation is that zirconium cations occupy positions left by substituent cations thus stabilizing the structure. At the same time, even with stabilizing cations, amorphous phases obtained by the sol–gel method followed by the hydrothermal treatment under conditions precluding crystallization remain amorphous upon the calcination at 900–1000°C. Hence, to obtain stable phases with a certain structure and reproducible properties, they should be formed in soft conditions.

Porous structure. For samples with a specific surface area ranging from 40 to 200 m^2/g (see the table), the total pore volume was in the range 0.1–0.5 cm^3/g, and the average pore diameter was in the range 40–260 Å [21]. Thus, dispersed framework zirconium phosphates synthesized by the hydrothermal treatment in the presence of polyethylene oxide are mesoporous systems, which is of particular importance for the long-chain hydrocarbon conversion.

2. ACID PROPERTIES OF SURFACE SITES OF FRAMEWORK ZIRCONIUM PHOSPHATES AND THEIR CONTROL VIA THE HETEROVALENT SUBSTITUTION IN THE LATTICE

It was found [18, 21, 24, 25] that surface groups of framework zirconium phosphates are largely represented by weakly acidic P–OH groups (the IR band at 3670 cm^{-1}), which experience disturbances by the low-temperature adsorption of CO. Samples synthesized using the MA method are characterized by a higher surface density of these groups probably due to the more developed close-packed basal faces (see above). Rather strong Brønsted acid sites were also found, which are represented by Zr–OH groups (the IR band at 3740 cm^{-1}). Lewis acid sites represented by coordinatively unsaturated Zr^{4+} cations were identified as complexes with CO at 77 K (the IR band at 2180–2200 cm^{-1}). The total surface concentration of all acid sites does not exceed 10% of the monolayer capacity, which allows their assign-

Methods of synthesis, phase compositions, and acid properties of the surface of framework zirconium phosphate samples

Sample*	Initial substances**	HTT conditions, pH/*T*,°C	Specific surface area, m^2/g	Intensity of the IR band of Zr–OH arb. u./g	$[Zr^{4+}]$, μmol CO/m^2	Phase composition (XRD data)***
MA-2	LaN + ZrCl + N3P	7/200	60	–	0.27	cub + rhomb
K-6	0.3%Pt + 10%W/MA-2	–	50	–	–	cub + rhomb
MA-3	LaN + N3P + ZrN	7/200	67	20	0.24	cub + rhomb
MA-5	ZrCl + N3P	7/200	40	–	0.13	cub + rhomb
MA-6	ZrCl + N3P + F	7/200	19	–	–	cub + rhomb + lamel
K-17	0.3%Pt/MA-6	–	19	–	–	
MA-7	ZrCl + N3P + B	6/200	56	–	–	cub + rhomb (trace)
K-18	0.3%Pt/MA-7	–	50	–	–	–
SG-1	LaN + ZrN + N2P	5/200	166	50	0.63	amorph
SG-6	ZrN + N2P	6/200	130	35	0.92	amorph + cub (trace)
SG-7	ZrN + N2P	1/200	28	–	1.3	rhbdr
SG-8	ZrN + N2P	3/200	114	25	1.18	amorph + rhbdr
SG-20	ZrBu	7/200	180	45	0.37	amorph
SiSG-21	ZrBu + TES	7/200	187	160	0.37	amorph
K-19	0.3%Pt/SiSG-21	–	180	66	0.27	amorph
SiSG-25	ZrBu + TES	7/100	158	71	1.14	amorph
SiSG-26	ZrBu + TES	7/200	165	76	0.97	amorph
K-26	0.3%Pt/SiSG-26	–	145	43	0.49	amorph
SiSG-30	ZrBu + TES + B	7/100	225	89	0.89	amorph
K-27	0.3%Pt/SiSG-30	–	193	–	–	amorph
SiSG-31	ZrBu + TES + F	7/100	29	––	0.79	lamel
K-28	0.3%Pt/SiSG-31	–	29	–	–	lamel

* Obtained by mechanochemical activation (the MA type), by the sol-gel method (the SG type), and by supporting noble metals onto MA- or SG-type samples (the K type).

** $La(NO_3)_3 \cdot 6H_2O$ = LaN, $ZrOCl_2 \cdot 8H_2O$ = ZrCl, $ZrO(NO_3)_2 \cdot 8H_2O$ = ZrN, $(NH_4)_3PO_4 \cdot 3H_2O$ = N3P, $(NH_4)_2HPO_4$ = N2P, $NH_4F \cdot HF$ = F, H_3BO_3 = B, ZrBu is zirconium butoxide, and TES is the tetraethyl orthosilicate.

*** Phases are abbreviated as follows: cub, cubic; rhomb, orthorhombic; rhbdr, rhombohedral; lamel, lamellar; and amorph, amorphous.

ment to surface defects. For all samples synthesized from inorganic substances by HTT in the presence of polyethylene oxide, the surface density of acid sites is much the same and higher than that for samples obtained by the MA method and those containing lanthanum (see the table).

It was found that the strongest Lewis acid sites ionize hexamethylbenzene molecules to yield radical cations detectable by ESR [21] but are inactive to more electronegative molecules, such as benzene and toluene. According to [26], these results indicate that the Lewis acid sites at the surface of framework zirconium phosphates are stronger than respective sites of γ-Al_2O_3 but weaker than those of sulfated aluminum oxide, HZSM-5, and zirconium dioxide.

The use of the TEMPON nitroxyl radical as a probe for strongest Lewis acid sites showed that, for samples obtained by the MA method, the proportion of these sites is greater than for samples obtained by the sol–gel method [24].

The influence of admixed ions in the structure of framework zirconium phosphates on the surface concentration of acid sites was studied in detail using organic precursors (see the table), because the controlled hydrolysis of these precursors enables the mixing of components at the atomic level. The introduction of silicon into the structure of framework phosphates in place of phosphorus increases the concentration of Brønsted acid sites (see the table), which can be explained in terms of a mechanism similar to that for the formation of acid sites in zeolites. The introduction of boron increases the Brønsted and Lewis acid site concentrations. With admixed fluorine, the density of Brønsted acid sites increases, and the density of Lewis acid sites decreases. The shielding effect of platinum and tungsten is indicative of their preferred binding with acid surface sites during the coating process [23, 25].

3. CATALYTIC PROPERTIES

In pulse-mode experiments, samples of framework crystalline phosphates without surface promoters, such

as tungsten and platinum, exhibit rather high activity and selectivity in the pentane and hexane isomerization reactions in the temperature range 450–550°C (the conversion is as high as 40–50%, and the selectivity with respect to isomers is 50–100%) [19, 24]. The initial activity correlates with the surface concentration of strongest Lewis acid sites. However, at steady-state conditions, these sites are deactivated due to the carbide formation; the result is a low activity in the temperature range 200–400°C, which is of practical interest.

The introduction of silicon into framework zirconium phosphates, as well as the modifying of their surface with tungsten and platinum, increases the steady-state conversion (to 30–40%) in the temperature range 250–350°C with retention of a high (about 80%) selectivity with respect to isomers [23, 25].

Framework phosphates with supported platinum metals promoted by transition metal oxides exhibit high activity and selectivity in the reaction of methane selective oxidation by oxygen into synthesis gas at short contact times [17]. They also show promise for the oxidative dehydrogenation of propane into propylene at short contact times [36].

REFERENCES

1. Clearfield, A. and Thakur, D.S., *Appl. Catal.*, 1986, vol. 26, p. 1.
2. Segawa, K., Kurusu, Y., Nakajima, Y., and Kinishita, M., *J. Catal.*, 1985, vol. 94, p. 491.
3. Frinaeza, T.N. and Clearfield, A., *J. Catal.*, 1984, vol. 85, p. 398.
4. US Patent 4384985.
5. McCormic, R.L. and Alptekin, G.O., *Catal. Today*, 2000, vol. 55, p. 269.
6. Ai, M., *Catal. Today*, 1999, vol. 52, p. 65.
7. Alamo, J. and Roy, R., *J. Mater. Sci.*, 1986, vol. 21, p. 444.
8. Hagman, L. and Kierkegaard, P., *Acta. Chem. Scand.*, 1966, vol. 22, p. 1822.
9. Alamo, J. and Roy, R., *J. Am. Ceram. Soc.*, 1984, vol. 63, p. 78.
10. Petkov, V.I., Orlova, A.I., and Egorkova, A.I., *Zh. Strukt. Khim.*, 1996, vol. 37, p. 1104.
11. Goodenough, J.B., Hong, H.J., and Kafalas, J.A., *Mater. Res. Bull.*, 1976, vol. 11, p. 173.
12. Roy, R., Vance, E.R., and Alamo, J., *Mater. Res. Bull.*, 1982, vol. 17, p. 585.
13. Alamo, J., *Solid State Ionics*, 1993, vols. 63–65, p. 547.
14. Chaikina, M.V., *Khim. Inter. Ustoich. Razvit.*, 1998, vol. 6, p. 141.
15. Komarneni, S., *Int. J. High Technol. Ceram.*, 1988, vol. 4, p. 31.
16. Clearfield, A., Roberts, B.D., and Subramanian, M.A., *Mater. Res. Bull.*, 1984, vol. 19, p. 219.
17. Pavlova, S.N., Sadykov, V.A., Paukshtis, E.A., *et al.*, *Stud. Surf. Sci. Catal.*, 1998, vol. 119, p. 759.
18. Sadykov, V.A., Kochubei, D.I., Degtyarev, S.P., *et al.*, *Mater. Res. Soc. Symp. Ser.*, 1998, vol. 497, p. 160.
19. Sadykov, V.A., Pavlova, S.N., Zabolotnaya, G.V., *et al.*, *Mater. Res. Soc. Symp. Ser.*, 1999, vol. 549, p. 255.
20. Pavlova, S.N., Sadykov, V.A., Zabolotnaya, G.V., *et al.*, *Dokl. Akad. Nauk*, 1999, vol. 364, no. 2, p. 210.
21. Pavlova, S.N., Sadykov, V.A., Zabolotnaya, G.V., *et al.*, *Phosph. Res. Bull.*, 1999, vol. 10, p. 400.
22. Sadykov, V.A., Pavlova, S.N., Zabolotnaya, G.V., *et al.*, *Mater. Res. Innov.*, 1999, vol. 2, no. 6, p. 328.
23. Sadykov, V.A., Pavlova, S.N., Zabolotnaya, G.V., *et al.*, *Mater. Res. Innov.*, 2000, vol. 3, p. 276.
24. Pavlova, S.N., Sadykov, V.A., Zabolotnaya, G.V., *et al.*, *J. Mol. Catal.*, 2000, vol. 158, no. 1, p. 319.
25. Pavlova, S.N., Sadykov, V.A., Zabolotnaya, G.V., *et al.*, *Stud. Surf. Sci. Catal.*, 2000, vol. 130, p. 2399.
26. Bolshov, V.A., Volodin, A.M., Zhidomirov, G.M., *et al.*, *J. Phys. Chem.*, 1994, vol. 98, p. 7551.
27. Shmachkova, V.P., Kotsarenko, N.S., and Mastikhin, V.M., *Kinet. Katal.*, 1994, vol. 35, no. 2, p. 314.
28. Kolomiichuk, V.N., *React. Kinet. Catal. Lett.*, 1982, vol. 20, p. 123.
29. Clayden, N.J., *J. Chem. Soc., Dalton Trans.*, 1987, p. 1877.
30. Mak, T.C.W., *Can. J. Chem.*, 1986, vol. 46, p. 3491.
31. Masse, R., Durif, A., Guitel, J.C., and Tordjman, I., *Bull. Soc. Fr. Mineral. Cristallogr.*, 1972, vol. 95, p. 47.
32. Ono, A., *J. Mater. Sci. Lett.*, 1985, vol. 4, p. 936.
33. Ono, A. and Okamura, F., *Bull. Chem. Soc. Jpn.*, 1985, vol. 58, p. 1051.
34. Chernoukov, N.G., Korshunov, I.A., and Zhuk, M.I., *Zh. Neorg. Khim.*, 1983, vol. 28, p. 1656.
35. Livage, J., *Catal. Today*, 1998, vol. 41, p. 3.
36. Sadykov, V.A., Pavlova, S.N., Saputina, N.F., *et al.*, *Abstracts of 6th Eur. Workshop on Selective Oxidation*, Rimini, 1999, p. 119.